Research Article

Vincent Ball*

Polydopamine films: Versatile but interface-dependent coatings

Abstract: Polydopamine coatings have been shown to allow to coat almost all materials with conformal films having a tunable thickness from a few up to more than 100 nm (and even more in some specific cases). These films are able to reduce metal cations, to be modified with many chemical moieties and advent hence as a "Holy Grail" in surface chemistry with an impressive amount of applicative papers published since 2007. However, the broad application field and ease of deposition from aqueous solutions hidden the complexity of the deposition mechanism(s). The discovery that polydopamine (PDA) films also form at air/water interfaces (in the absence of stirring or in stirring dependent manner) to yield membranes with physicochemical properties different than PDA films deposited at solid/water interfaces highlighted for the first time that the nature of the interfaces plays a major role in the PDA film growth mechanism and in the film properties. More recent research allowed to show that the surface chemistry of the used solid substrate modifies the composition of the thin deposited PDA film during the early stages of the deposition process with further deposition yielding to an almost substrate-independent PDA film. It is the aim of this review to describe complex surface effects occurring in PDA deposition and hence to complement other reviews which described the complexity of the chemistry yielding to PDA coatings.

Keywords: polydopamine, polydopamine films, PDA coatings

* **Corresponding author: Vincent Ball**, Faculté de Chirurgie Dentaire, Université de Strasbourg, 8 rue Sainte Elisabeth, 67000, Strasbourg, France; Institut National de la Santé et de la Recherche Médicale, Unité Mixte de Recherche 1121, 1 rue Eugène Boeckel, 67084, Strasbourg, France, e-mail: vball@unistra.fr

1 Introduction

For a long time, the functionalization of the surfaces of materials with robust and functional coatings was substrate specific with functionalization protocols specific for metallic surfaces [1] and oxides [2] and much less possibilities for the surfaces of polymers. The bio-inspiration from mussels which adhere to many different substrates (wood, stones, *etc.*) in wet conditions and in the presence of strong shear stresses allowed to introduce polydopamine (PDA) coatings in surface science [3]. The idea to use dopamine was the simultaneous presence of catechol and amine functions in the same molecule whereas the same groups are present in the mussel foot proteins as separated side chains, L-DOPA (a hydroxylated L-tyrosine residue) and L-lysine, respectively [4].

PDA films found their broadest field of applications for substrate-independent postfunctionalization, not only by PDA itself but also by using the chemical reactivity of PDA [5,6] to graft molecules like polypeptides at its surface [7], to induce polymerizations [8,9] or to deposit metallic particles through the reducing power of PDA [3], and to complexation of metal cations in water purification [10]. PDA films on sacrificial polymeric or oxide particles allow to form hollow capsules for applications like controlled drug delivery after specific functionalization of the PDA shell [11]. Along with all the possible applications of PDA coatings, their broad catalytic properties [12–15] seem to be underexploited.

The preparation of PDA films is straightforward: the substrate to be coated has simply to be dipped in an aqueous dopamine solution at a slightly basic pH value and in the presence of dissolved oxygen which oxidizes dopamine in dopamine quinone, the first step of a complex reaction mechanism yielding to 5,6-indolequinone the polymerization/self-assembly thereof yielding to PDA. Later on, the deposition of PDA films from solutions at different pH values and using other oxidants than dissolved oxygen was described [16,17]. The factors allowing to tune the deposition of PDA films, notably the nature of the available buffer [18,19] as well as the different deposition methods, are now mainly known and reviewed [20].

Despite the enormous number of papers published in this field, the mechanism(s) leading to PDA films at interfaces and to PDA precipitates in solution remain largely hypothetical [21–23] mainly due to the absence of solubility of the obtained material in analogy with its natural analog: eumelanin [24]. At the present stage, the most probable structure of PDA seems to be a mixture of polymeric domains and domains containing small oligomers of 5,6-dihydroxyindole (DHI) or some dopamine$_2$-DHI clusters [25].

Even if PDA films form at the surface of almost all materials, some recent findings point to situations where no PDA deposits on silica in a DMSO-phosphate buffer saline mixture (1:1, v/v) [26] or where the structure of the substrate influences the composition and structure of the obtained coating. This adds additional complexity in those films and materials. It is the aim of this review article to describe the actual state of knowledge about the influence of the substrate, or the nature of the interface on the deposition kinetics, deposition mechanism, composition, and structure of the obtained PDA films. This article is issued from discussions which occurred during the "second Polydopamine symposium" October 11–12, 2023, in Poznan. The first section will deal with PDA deposition at the air–water interface. The second section will deal with some peculiar aspects of the PDA formation in the presence of interfaces of biological significance: the interface between biomolecules (mostly proteins) and dopamine containing solutions. The three last sections will be devoted to the solid–liquid interfaces highlighting the influence of the surface chemistry and the use of a conductive material to deposit PDA through electrodeposition, respectively. The influence of the oxidant used to form PDA coatings on the PDA-aqueous solution interface will also be discussed. Finally, taking all the findings summarized herein into account, a nomenclature will be proposed to help identify interfacial effects in the obtained films' composition and structure

2 PDA at the air–water interface

If PDA coatings are deposited at all kinds of interfaces, they should also form at the air–water interfaces. This was not reported before 2014, because most investigators synthesize PDA under strong agitation of dopamine solutions to provide oxygen supply to the solution. But in the absence of strong shear forces at the air–water interface, a PDA film forms there through autoxidation of dissolved dopamine [27]. The formation of PDA membranes at the air–water interface is preceded by a lag phase as found by bubble tensiometry (Figure 1a). This finding strongly suggests that
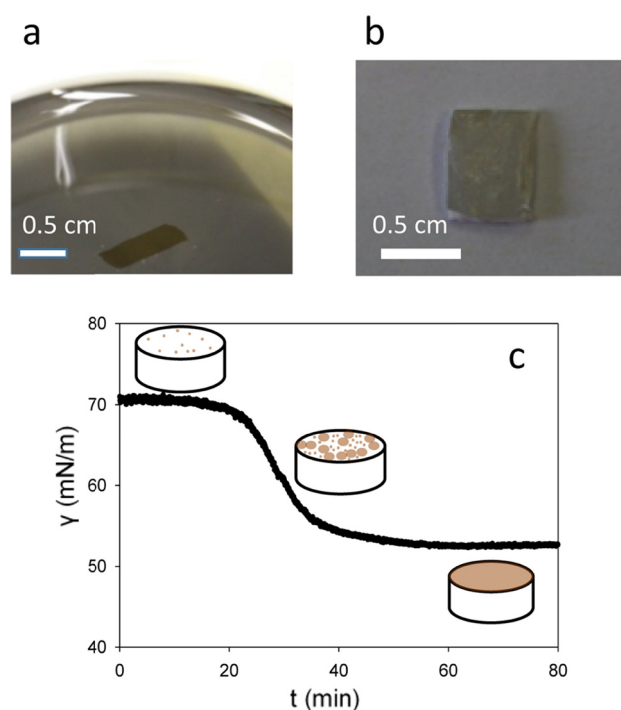

Figure 1: Pictures of a PDA free-standing film at the air–water interface after the Langmuir Schaeffer transfer on a quartz slide (a) and on a piece of PTFE after transfer from the air–water interface (b). (c) Evolution of the surface tension *versus* time in a pendant drop configuration. The dopamine concentration in the Tris buffer was of 2 mg mL^{-1} inside the water droplet. The schemes in the insets depict the progressive coverage of the air–water interface with PDA particles leading to a homogeneous film after their 2D growth and coalescence. Reproduced with authorization from [27].

the oxidation process of dopamine in solution leads to the formation of amphiphilic species which adsorb at the air–water interface and self-assemble there to produce nuclei of a critical size from which PDA film growth occurs [27]. This is totally different from the deposition of PDA at the solid–liquid interface where the film starts to grow immediately after contact between the dopamine solution in the presence of O$_2$ and the solid substrate [3].

The films obtained at the air–water interface could be transferred on solid substrates, silicon wafers, and PTFE foils through the vertical Langmuir Schaefer Method (Figure 1b). The film thickness increased linearly with time at least up to 4 h and was found to be much higher than the thickness of the films deposited at the silicon–water interface in the same conditions (aerated solution in the presence of 50 mM Tris buffer at pH = 8.5). This increase in film thickness with respect to the film thickness at the solid–liquid interface may simply be due to a higher oxygen supply. But it has to be noted that PDA films at the air–water interface can also be obtained at pH = 5.0, where the rate of

autoxidation is negligible even in the presence of dissolved oxygen, using sodium periodate as the oxidant [28].

The dynamic surface elasticity of PDA films at the air–water interface from dopamine solutions (0.5–5.0 mg mL^{-1}) in 10 mM Tris buffer was found to be maximal (60 mN m^{-1}) for a dopamine concentration of 1.0–1.5 mg mL^{-1} after two hours of film formation [29]. The dynamic surface elasticity, defined as the ratio between the infinitesimal change in surface tension and in the relative surface area as obtained by oscillating a ring vertically at the interface and measuring the resulting periodic change in surface area, decreased for higher initial dopamine concentrations. However, the film thickness (as measured by ellipsometry at the air–water interface) continued to increase from about 60 nm at 1 mg mL^{-1} in dopamine to about 115 nm at 5 mg mL^{-1} in dopamine after 15 h of deposition [29]. These thickness values are again much higher than those obtained in the same physicochemical conditions but on a solid–liquid interface.

Water droplets coated with a PDA film undergo a shape transformation from a dome to a flat surface due to partial evaporation of water. This change in shape is reversible when water is reinjected in the droplet [30] and is a consequence of the elasticity of the PDA film.

The thickness of PDA membranes grown in the presence of Tris buffer (at pH = 7.5, 8.0, and 8.5) at the air–water interface was measured directly at the water surface using reflectance measurements. These data were compared with those obtained by AFM after transfer of the membranes at silicon substrates and both kinds of measurements were in excellent agreement (Figure 2) [31]. Since the dopamine solution was stirred with a magnetic stirrer placed in the center of the Petri dish, the obtained thicknesses were significantly smaller than those obtained without agitation [27]. In the membrane region above the magnetic stirrer, the PDA film thickness was systematically smaller than in the external part of the Petri dishes the more so the higher the dopamine concentration (which was varied between 0.5 and 2 mg mL^{-1}) at pH 7.5. Synthesis performed at pH 8.0 under stirring at 300 rpm with an initial dopamine concentration of 0.5 mg mL^{-1} allowed to obtain smooth membranes with small thickness variation between the center of the Petri dish and far away from it (Figure 2).
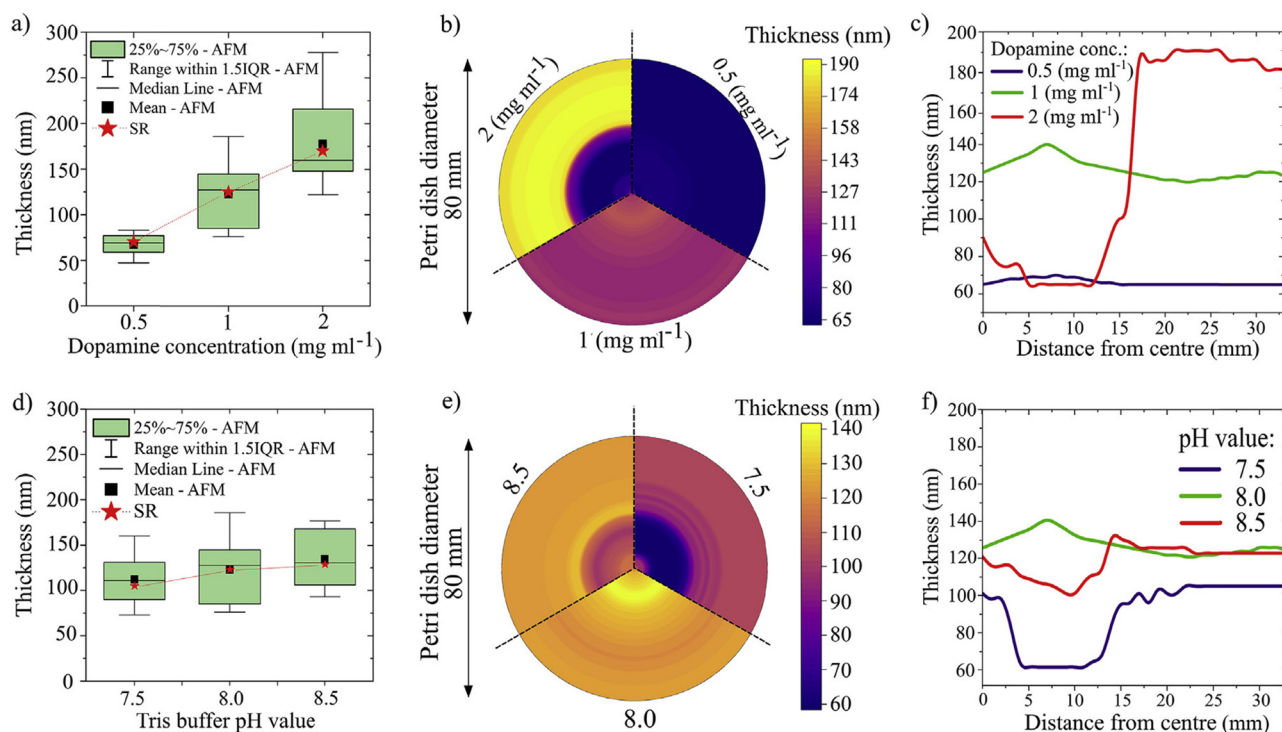

Figure 2: (a) Influence of the dopamine concentration (in Tris buffer at pH = 8.5) on the thickness of PDA free-standing films as measured by AFM (Boxes) and optical reflectometry (Points). (b) Radial mapping (with a resolution of 1 mm) of the film thickness for different dopamine concentrations as determined by optical reflectometry. (c) Line chart of film thickness of free-standing PDA films at different dopamine concentrations along the radius of the Petri dish as determined by optical reflectometry. (d) Influence of the pH of the Tris buffer on the thickness of the free-standing PDA films at a constant initial dopamine concentration of 1.0 mg mL^{-1}. (e) Radial mapping of the free-standing PDA film thickness as a function of the pH value of the Tris buffer. (f) Line chart of film thickness as a function of the pH values of the Tris buffer. Reproduced with authorization from [31].

The structural and mechanical properties of the PDA films taken from the air–water interfaces were also investigated [32]. The PDA free-standing films produced from dopamine solutions at $2\,mg\,mL^{-1}$ (in 10 mM Tris buffer, pH = 8.5) displayed the presence of several sheets about 50 nm in thickness and their X-ray diffraction patterns contained a set of peaks at about 2θ = 10.7, 21.6, 32.4, and 41° values which are close to those obtained with carbon-based materials [33]. This finding is surprising because the PDA free-standing films did not underwent a thermal treatment before their characterization.

Analysis of the peak width allowed to estimate the size of those crystalline domains to some tens of nanometers. This finding should be put in relation with the observation of onion-like structures with an interplanar spacing of 0.34 nm [34,35], typical of ordered carbon materials but not (yet) observed in thin PDA films deposited at the solid–solution interface. This is an additional illustration that PDA deposited at the air–water interface may be structurally different from PDA deposited at solid–liquid interfaces. In addition, nanoindentation measurements performed on the films taken from the air–water interface gave a Young modulus of 13 ± 4 GPa and a hardness of 0.21 ± 0.03 GPa, surprisingly high values for a polymer-based material [32]. After the addition of boric acid to the dopamine solution, the Young modulus of the PDA membranes at the air–water interface could be increased to 18.3 ± 6.4 or 24.1 ± 5.6 GPa using Brillouin light scattering and nanoindentation as the measurement method respectively [36].

PDA membranes obtained at the air–water interface and PDA particles obtained from the same dopamine solution but in the presence of either NaCl, $MgCl_2$, $CaCl_2$, or $CoCl_2$ at 100 mM were compared for their composition [37]. The PDA membranes obtained in the presence of Co^{2+} cations were much thicker (as determined from their cross-section by means of SEM) than their counterparts obtained in the presence of either Na^+, Mg^{2+}, or Ca^{2+} (Figure 3a). It appeared that, whatever the used cation, the films were enriched in carbon with respect to the nanoparticles, suggesting higher oxygen incorporation in the nanoparticles compared to the film. The PDA nanoparticles are indeed enriched in oxygen, nitrogen, and metallic cations with respect to the free-standing films. This is, to the best of the author's knowledge, the first example in the literature suggesting that the formation mechanism, and finally the final structure and composition of PDA are different in solution and at the water–air interface. Additionally, the presence of Co^{2+} cations accelerated the growth of the PDA membranes at air–water interface. Finally, whatever the used salt, the water contact angles of the membrane

side exposed to the air were higher than the corresponding contact angle at the side exposed to the dopamine solution [37]. This may well be related to changes in composition but also to changes in the roughness of the membrane. The membranes obtained from Co^{2+} containing dopamine solutions were more hydrophilic (Figure 3b) than those obtained in the presence of the other investigated cations [37]. The free-standing films containing Co^{2+} cations seem much less brittle than those produced in the absence of metallic cations.

To improve the mechanical properties of PDA-based free-standing films the idea was, from the beginning on, to add some reactive polymers-containing nucleophilic groups able to crosslink PDA-in the subphase [38] (Figure 4). Poly(ethylene imine) in the subphase allowed to produce robust and thick membranes at the air–water interface. Those membranes made from either dopamine, norepinephrine, pyrocatechol or 3,4-dihydroxyhydrocinnamic acid were also strongly adhesive to the reaction beaker. This strong adhesion allowed to withstand the solution's own weight (Figure 4a). The mechanical properties of those membranes were evaluated directly at the air–water interface using U-tubes made either from silicon rubber or PVC (Figure 4b–d). The membranes kept the ability of PDA to reduce Ag^+ into silver nanoparticles (Figure 4e) and displayed an asymmetric Janus-like structure with a PDA-rich composition at the membrane air–interface and a PEI-rich composition at the membrane–solution interface (Figure 4g and h) [38].

Smaller PEI molecules ($600\,g\,mol^{-1}$) allowed also to produce composite free-standing films from the air–water interface with a final thickness ranging from 80 nm to 1 μm depending on the experimental conditions, namely the reaction time and the dopamine/PEI ratio in the reaction mixture [39].

Polymers like alginates modified with catechol groups (alg@cat) can also be used to reinforce PDA membranes at the air–water interface [40]. In this case, the catechols linked as side chains on the polymer (grafting ratio close to 10%) are expected to crosslink with PDA during the simultaneous oxidation of both compounds. High-resolution N1s X-ray photoelectron spectroscopy (XPS) allowed to show that the composition of the solution side of the membrane was slightly depleted in pyrollic groups when compared to the air side. Interestingly, the UV–Vis spectrum of the film transferred from the air–water interface (80 μm in thickness as determined from the cross-section after imaging by SEM) on a quartz slide was totally different than the UV–Vis spectrum of PDA directly deposited from the dopamine solution in the same conditions (dopamine at $2\,mg\,mL^{-1}$ in the presence of 50 mM Tris buffer
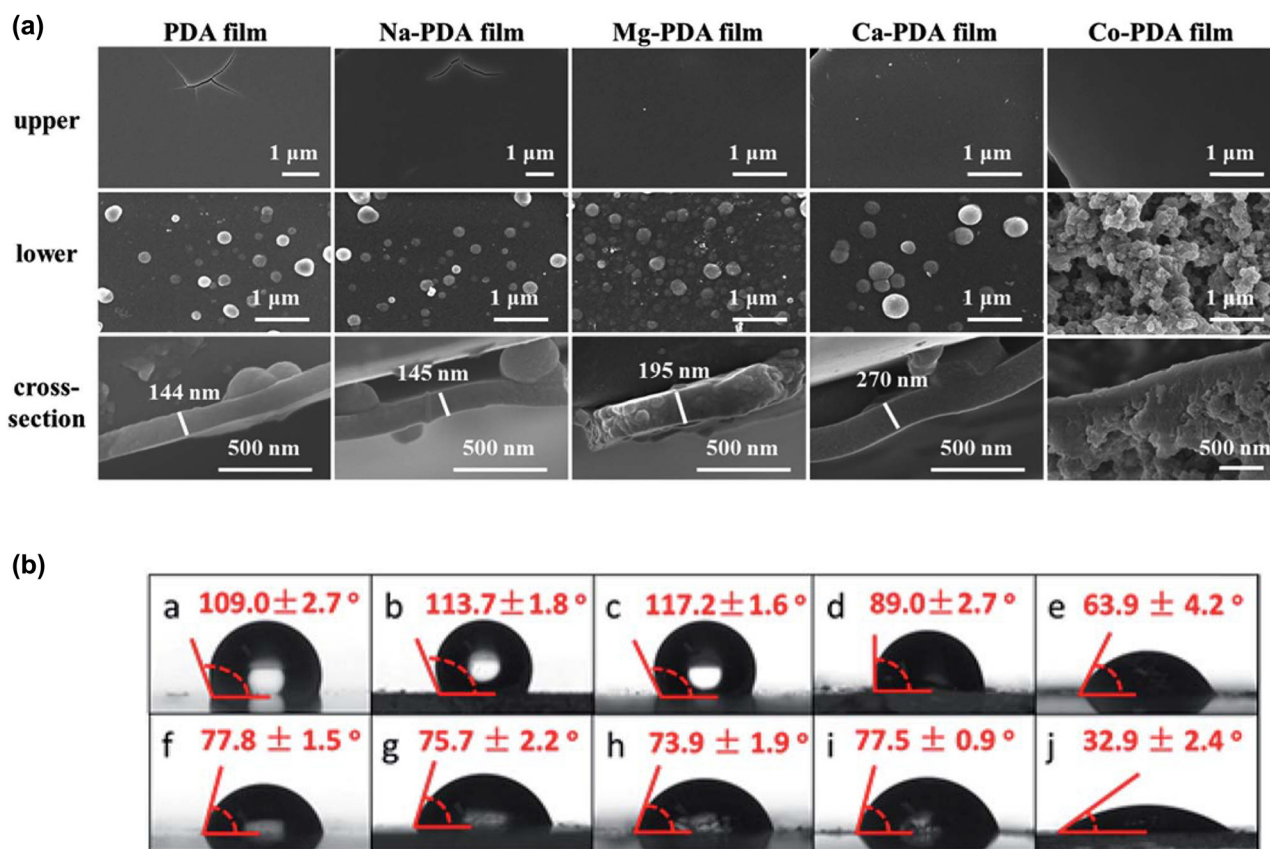
(a)

(b)

Figure 3: (a) SEM images of PDA free-standing films produced in the presence of different metal ions (salt concentration equal to 100 mM), compared with free-standing films produced in the absence of added salt. The pictures in the first line were taken from the upper surfaces of the free-standing films, namely the surfaces exposed to air whereas the pictures in the second line were taken from the lower surfaces of the free-standing films exposed to the solutions during the synthesis. The pictures in the third line are cross-sections of the free-standing films in order to determine their thickness. All PDA films were obtained after 2 days of reaction from 10 mM dopamine solution dissolved in 10 mM Tris buffer at pH = 8.8. (b) Water contact angles of the upper surfaces (images a–e) and lower surfaces (images f–j) of PDA free-standing films generated from 10 mM dopamine solution (10 mM Tris buffer pH = 8.8) in the presence of different salts (100 mM) after 24 h reaction. PDA without added salt (a and f); PDA produced in the presence of NaCl (b and g), PDA produced in the presence of $MgCl_2$ (c and h); PDA produced in the presence of $CaCl_2$ (d and i); and PDA produced in the presence of $CoCl_2$ (e and j). Reproduced with authorization from [37].

pH = 8.5 with dissolved O_2). Namely, the spectrum from the deposited free-standing film exhibited a broad peak at around 550 nm, whereas those μm thick films exhibited no structural color [40]. This interesting finding deserves more fundamental investigations and may be related to a change in composition induced by the air–water interface, for instance a selective extraction from the solution of some species produced from the dopamine oxidation and the crosslinking product thereof with alg@cat.

When the PDA-based films at the air–water interface are produced in the presence of laccase, their interfacial elasticity (400 mN m^{-1}) is improved with respect to that of the films produced from the autoxidation of dopamine in the same experimental conditions (about 75 mN m^{-1}) [41]. This particular example is an illustration that the presence of biopolymers, developing an interface with water, can

play a major role in the formation of PDA and in its properties.

3 PDA at biological interfaces

Eumelanins in the skin appear not only as pretty homogeneous and hierarchical aggregates [42] but they are also surrounded by proteins [43,44]. However, when synthetic eumelanin or its analog PDA is produced in solution, they often form large heterogeneous aggregates which precipitate from the solution, the more so the higher the solution concentration of the precursor. This difference between biogenic melanins and synthetic analogs, among them PDA, suggests that the protein–dopamine solution
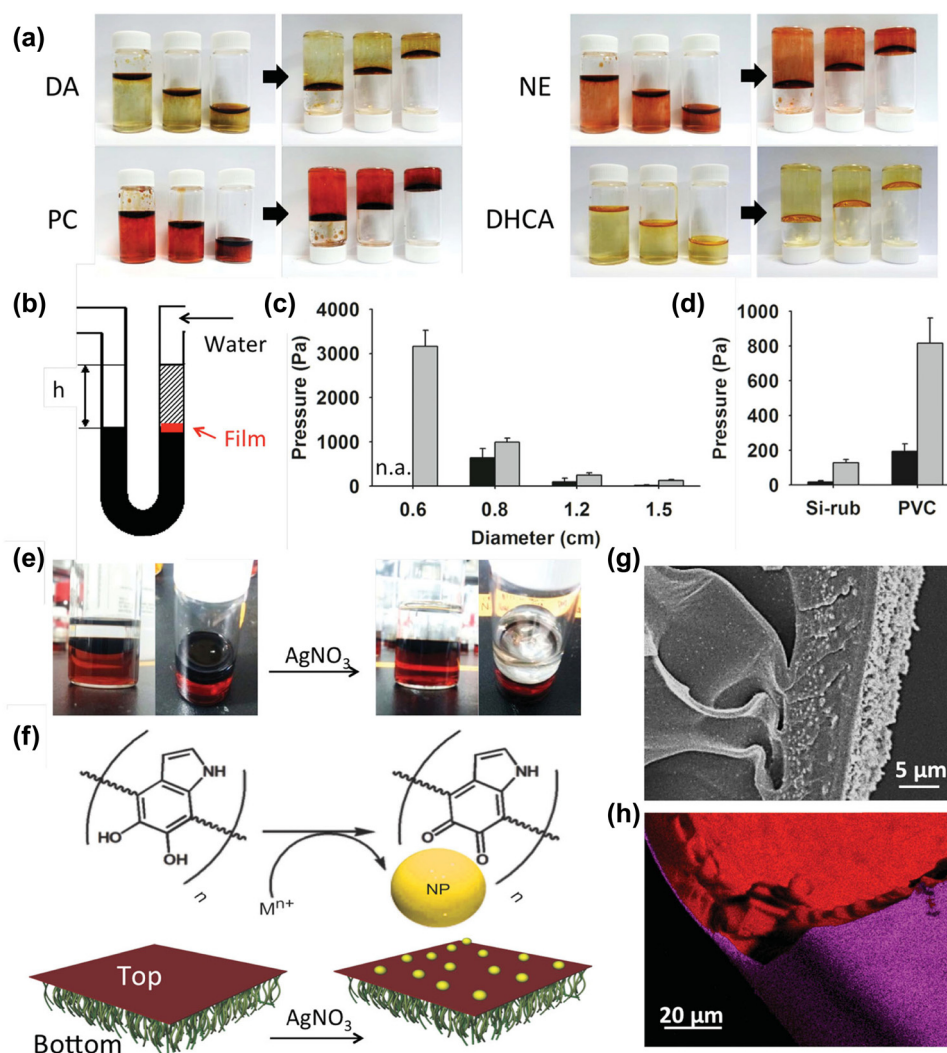
Figure 4: The adhesive properties of free-standing catecholamine-based films. (a) Pictures of the air–water free-standing films prepared from dopamine (DA, upper left), norepinephrine (NE, upper right), pyrocatechol (PC, lower left), and 3,4-dihydroxyhydrocinnamic acid (DHCA, lower right) in the presence of PEI in the subphase. All the films were able to withstand the weight of the solution owing to their strong adhesion to the glass vial. (b) Design of a U-shaped tube to measure maximal endurance pressure. (c) Maximal endurance pressure of the PEI/DA films attached to silicone rubber-based U-shaped tube. Gray bars: data from the films prepared for 24 h, black bars correspond to films prepared during 4 h. (d) Material-dependence of maximal endurance pressure on silicone rubber and poly(vinyl chloride) (PVC) U-shaped tubes. (e) Change in the visible appearance of the upper side of the free-standing films after exposure to a silver nitrate solution. (f) Scheme illustrating the metal cation reduction and nanoparticle formation on the top side of the catecholamine free-standing films. (g) Cross-sectional SEM view of the silver-decorated Janus film. (h) Elemental mapping of the anisotropic film obtained after the reduction of Ag$^+$ cations. Carbon appears in red whereas silver appears in purple. Reproduced with authorization from [38].

interface plays a role in the formation of PDA. Indeed, in the presence of the whole protein pool from egg yolk, the oxidation of DHI yields the formation of monodisperse PDA-like particles with an average diameter between 15 and 65 nm [45]. Similarly, when dopamine is oxidized in the presence of human serum albumin (HSA) (at pH = 8.5 in the presence of 50 mM Tris buffer), monodisperse PDA particles are formed with a size (measured by dynamic light scattering) decreasing upon an increase in the protein/dopamine ratio [46]. But other proteins like hen-egg white lysozyme or bovine α-lactalbumine do not influence the formation of PDA aggregates or the deposition of PDA on the walls of the reaction vessel. Hence, such kinds of proteins are spectators in the dopamine oxidation and PDA formation. The influence of certain proteins on the formation of controlled PDA nanoparticles and the absence of influence of others required some fundamental investigations to understand the underlying mechanisms. Instead

of additional trial and error experiments, biological systems other than the skin melanocytes containing catecholamines and proteins are appropriate to select molecules able to play a role in the dopamine oxidation-self-assembly process. The adrenal medullary chromaffin cells were selected as such a biomimetic system: the chromaffin vesicles these cells emit are rich in catecholamines and proteins such as chromogranins [47]. The controlled hydrolysis of those proteins yields a large repertoire of polypeptides whose interactions with dopamine in oxidizing conditions were investigated. When a dopamine solution was allowed to undergo oxidation in the presence of such peptides (at a constant dopamine/peptide molar ratio of 10 in the presence of 50 mM Tris buffer at pH = 8.5), the ones containing a KE diad (K: L-lysine; E: L-glutamic acid) allowed to produce PDA aggregates able to elute in a time greater than the dead volume in a size exclusion chromatography experiment. However, polypeptides devoid of the KE diad produced aggregates that eluted with the dead volume in such screening experiments [48]. These findings were confirmed with smaller synthetic peptides, in which the KE diad was surrounded by some glycine residues or peptides in which K and E were separated by one or two glycine spacers. Molecular dynamic simulations were performed to investigate the interactions between non-oxidized dopamine and the GGKEGG, GGEKGG, and GGKGEGG peptides and also for the GGKDGG sequence. In pure water, the interaction time between GGKEGG and dopamine was the longest, 0.246 ns, and decreased dramatically to 0.131 ns upon an inversion of the position of K and E in the amino acid sequence, namely for the GGEKGG sequence. The replacement of glutamic acid (E) by the shorter residue of aspartic acid (D) has also a marked negative influence on the residence time of dopamine with the peptide. Considering the interactions between dopamine and the peptide, it appears that dopamine forms preferential hydrogen bonds with the carboxylic acid of glutamic acid than with the C terminal carboxylic acid, which is located further away (2 glycine residues). At the same time, the protonated amine of the lysine residue establishes a cation–π interaction with the benzene ring of dopamine [48]. These simulations suggest that dopamine interacts preferentially with the peptide–solution interface and undergoes preferential oxidation there than in the bulk of the solution. It was then noted that HSA which allows to control the size of the PDA nanoparticles in a dose-dependent manner [46] contains two solutions exposed KE diads in its amino acid sequence, whereas the inactive hen egg white lysozyme and bovine α-lactalbumine do not contain consecutive K and E residues in their primary structure. This incited to investigate the role of other KE containing proteins in the control of the size of PDA-based nanoparticles:

bovine fibrinogen, alkaline phosphatase (ALP), and a mixture of glucose oxidase (GOX) and peroxidase (POX) were found to contain 2, 3, and 1 + 1 KE residues, respectively. All of these proteins allowed to control the size of PDA nanoparticles synthesized in their presence (dopamine at $2\,mg\,mL^{-1}$) and to reduce PDA deposition on the wall of the reaction beaker and on quartz wafers immersed in the reactive medium. Figure 5 illustrates the influence of an increasing concentration in alkaline phosphatase on the deposition of PDA films (Figure 5a) and the size of the obtained PDA nanoparticles (Figure 5b and c) [48].

Finally, owing to their negative surface charge at pH = 8.5, the obtained composite PDA nanoparticles, made in the presence of ALP and the GOX + POX mixture, were deposited in alternation with the positively charged poly(allylamine hydrochloride) to yield films on silicon substrates. Those films kept the enzymatic activity of ALP and of the GOX + POX respectively [48,49]. This finding suggests that the PDA nanoparticles produced in the presence of ALP or GOX + POX expose some active enzymes at the particle–solution interface. Those non-cytotoxic nanoparticles (as tested against mouse macrophages and human fibroblasts) [48] could be used for biosensing applications in the future. Some additional investigations with other proteins and enzymes aiming to control the formation of PDA nanoparticles need however to be performed.

Similar PDA nanoparticles produced in the presence of transferrin were able to penetrate in mouse melanoma cells which overexpress transferrin receptors. This finding is additional evidence that some transferrin is incorporated in the PDA nanoparticles and that part of the protein is exposed at the nanoparticle–solution interface [50].

Another way to use the protein–solution interface is to adsorb mushroom tyrosinase to a solid substrate and to put the adsorbed protein layer in contact with an L-DOPA solution at different concentrations (with the addition of $CuSO_4$ at 5 μM): the adsorbed enzyme allowed to control the formation of eumelanin like particles 30–60 nm in diameter only at locations where the enzyme was adsorbed [51].

The interaction between biopolymers and catecholamines is specific in most cases [48,52], but polymers like poly(vinyl alcohol) also have a non-specific influence on the aggregation of the particles formed during the polymerization of DHI (12.5 μM in phosphate buffer at pH 7.0 using horseradish peroxidase [$25\,U\,mL^{-1}$] and H_2O_2 [12.5 mM] as the oxidant) [53]. Small angle neutron scattering data allowed to show that the internal organization of the material constituting the obtained particles was not affected by poly(vinyl alcohol) (up to 1.5 wt%) suggesting that the polymers adsorb on the formed nanoparticles impeding their further aggregation into μm sized aggregates, which
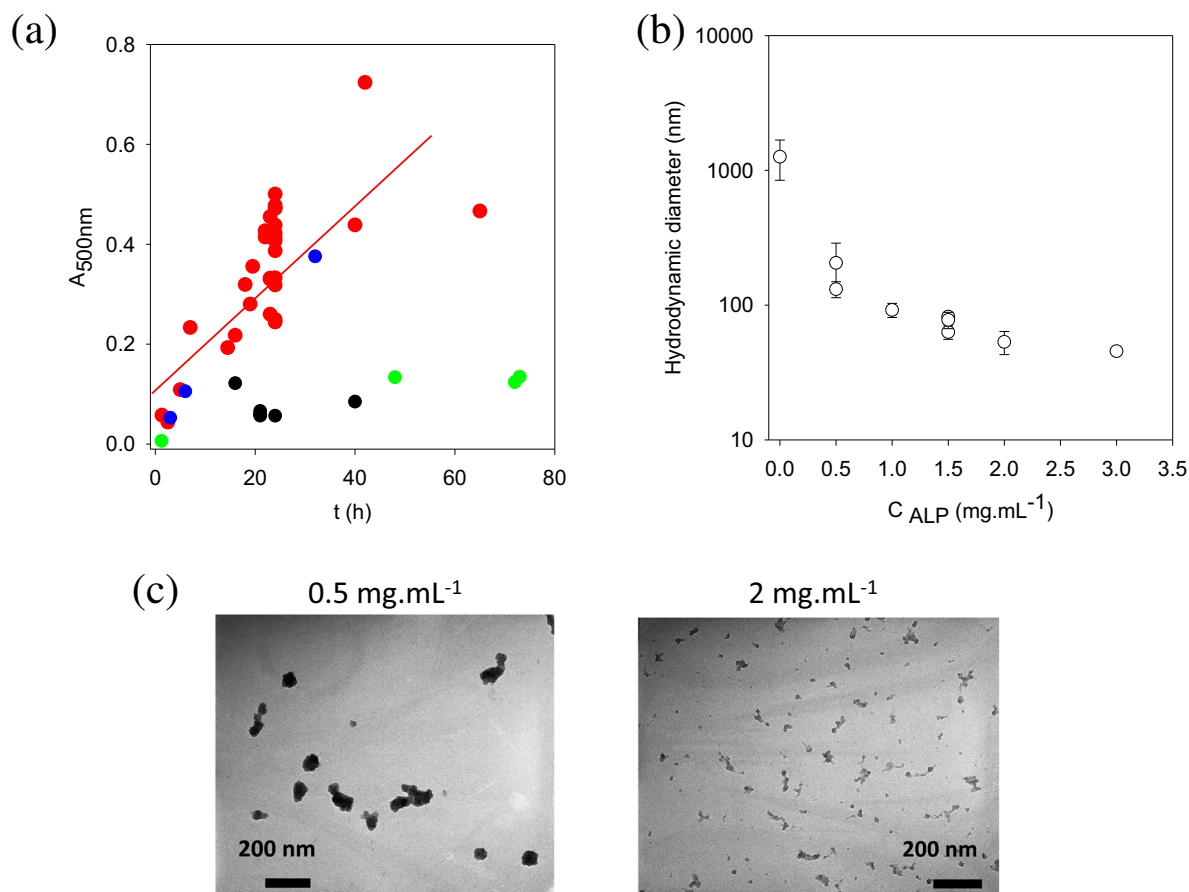
Figure 5: (a) Deposition of PDA films on quartz plates (monitored at λ = 500 nm) as a function of the oxidation time at pH = 8.5 (50 mM Tris buffer): in the absence of Alkaline phosphatase (ALP) (red disks ●) and in the presence of the enzyme at 0.1 (green disks ●) and 0.5 (black disks ●) mg mL^{-1}. Alkaline phosphatase was also preadsorbed during 1 h from a solution at 1 mg mL^{-1} before the beginning of dopamine oxidation but in the absence of ALP (blue disks ●). (b) Evolution of the hydrodynamic radius of PDA particles after 24 h of oxidation at pH = 8.5 (50 mM Tris buffer) in the presence of Alp at different concentrations. The initial dopamine concentration was equal to 2 mg mL^{-1} in all those experiments. (c) TEM micrographs of the PDA@ALP particles obtained after 24 h of oxidation at pH = 8.5 (50 mM Tris buffer) from a dopamine solution at 2 mg mL^{-1} in the presence of the enzyme at 0.5 and 2.0 mg mL^{-1} highlighting the reduction in particles' size upon an increase in the enzyme concentration also observed by means of dynamic light scattering (part b). Reproduced with authorization from [48].

are otherwise obtained in the absence of the capping polymer [53].

Some surfactants (like sodium dodecyl sulfate and hexadecyltrimethylammonium bromide) allow also to control the size of PDA nanoparticles obtained at pH = 8.5 (O$_2$ as the oxidant in Tris buffer) at a surfactant concentration above their critical micellar concentration. This finding suggests a preferential formation of PDA inside the micelles or at the micelles–solution interface [54]. Some other surfactants like Triton X100 (a non-ionic surfactant) are however inefficient in controlling the size of PDA formed in solution. Clearly, some more investigations are required in this field. The situation is identical for polyelectrolytes [55]. Indeed, polycations as well as polyanions have been found to allow the control of the size of PDA nanoparticles in the 10–100 nm diameter range. In particular, poly(allylamine hydrochloride) (PAH) adsorbs on the surface of PDA to reverse its zeta potential from negative (about −20 mV for PDA aggregates in the absence of PAH at pH = 7) to positive (reaching a plateau of +35 mV at the same pH when the initial PAH concentration is above 5 mg mL^{-1}). Simultaneously, above a threshold ratio of 0.7 polyelectrolyte monomer unit per dopamine monomer, this polycation inhibits the deposition of PDA at the solid–water interface since no observable deposit is formed at the surface of the used reaction vessel and on silicon wafers present in the reaction vessel [55]. On the basis of these results, it was assumed that dopamine oxidation and subsequent polymerization/self-assembly into PDA occur preferentially on the polycation–solution interface. Owing to the

presence of uncharged primary amino groups on PAH (particularly at pH = 8.5 in the presence of 50 mM Tris buffer), the occurrence of Michael adducts or Schiff bases with quinone groups present on PDA or small oligomers of dopamine cannot be excluded. Indeed, PAH interferes with the formation of PDA owing to a faster increase in the absorbance of the dopamine solution in the presence of PAH at 5 mg mL^{-1} at low reaction times (dopamine at 2 mg mL^{-1}). However, poly(diallyldimethylammonium chloride) carrying only quaternary ammonium groups allows also for the stabilization of nanosized PDA [55] without being able to form covalent adducts with it. When PDA is produced in the presence of polyarginine, also able to establish covalent bonds with oxidized moieties on PDA, nanoparticles stable against aggregation were obtained. The polyarginine present on their surface conferred them with antimicrobial properties [56].

4 Influence of the substrate in the initial deposition of PDA at solid–liquid interfaces

The versatility of PDA and related catecholamine-based materials to coat the surfaces of almost all known materials is well documented and certified [3]. Some detailed investigations highlight however the marked influence of the surface chemistry of the substrate on the initial stages of the film growth process.

Bettinger *et al.* [57] investigated the PDA film morphology and growth kinetics (from 2 mg mL^{-1} dopamine solution in the presence of 50 mM carbonate–bicarbonate buffer with pH changing from 8.2 to 10.0) on silicon oxide and on silicon modified with self-assembled monolayers, namely 3-aminopropyltrimethoxysilane- ($-NH_3^+$), phenyltricholorosilane- (–Ph), and octadecyltrichlorosilane- (–CH$_3$) based monolayers. It was found that:
1) The average size of the islands (measured by AFM in tapping mode) on the film increased in the following sequence: –CH$_3$ ~ –Ph < ($-NH_3^+$) < –SiO$_2$ (Figure 6a)
2) The number of islands per unit surface area (determined from image analysis) increased logically in the reverse order.
3) The number of islands per unit surface area scaled linearly with the maximal PDA deposition rate (Figure 6b) as determined by quartz crystal microbalance with dissipation monitoring.

The authors interpreted these data as being related to different modes of interaction between dopamine and its oxidation products with the moieties present at the surface of the substrate: hydrogen bonds but electrostatic repulsion with –SiO$_2$, electrostatic attraction and cation π interaction with ($-NH_3^+$), π–π, and hydrophobic interactions with –Ph and –CH$_3$ terminating monolayers [57]. The hydrophobic ending monolayers seem to induce a greater nucleation rate and hence more deposited islands per unit area at the end of the deposition step (Figure 6b).

The deposition of PDA films on hydrophobic polymer surfaces [58], namely poly(vinylidene fluoride) (PVDF), polytetrafluoroethylene, poly(ethylene terephthalate) (PET), and polyimide, was only slightly dependent on the used substrate in quite good agreement with the data of Bettinger *et al.* [57].

The early stages of PDA deposition on template-stripped gold electrodes from dopamine solutions at 1 mg mL^{-1} in 100 mM carbonate–bicarbonate buffer at pH = 8.5 have been investigated by a combination of experimental techniques including AFM, electrochemistry, and XPS [59]. It was found that a conformal film was formed only after 10 min of deposition whereas an island morphology was characterized after 2 and 5 min of deposition. Interestingly, XPS showed a change in the film composition for short deposition times when compared to longer durations. In particular, the percentage of tertiary amines was much higher at the initial stages of deposition whereas the percentage of secondary amines was much lower than at later stages. One should wonder if this change in composition originates from a substrate effect or from a change in film composition due to the deposition of particles from the solution which have been produced during longer oxidation-self-assembly. Indeed, in this investigation as in many others, it is assumed that PDA film forms from the deposition of species produced in solution. This assumption should be severely questioned in future investigations owing to the results obtained by Bettinger *et al.* [57].

The deposition kinetics of PDA (2 mg mL^{-1}, from Tris buffer at pH = 8.5) as followed by spectroscopic ellipsometry was much faster on PVDF (spin coated on silicon oxide) than on silicon oxide at all the three investigated temperatures, namely 20, 30, and 45°C [58]. At 20°C, the PDA film thickness on silicon oxide was equal to 24 nm, much less than the 49 nm obtained on PVDF. In the same investigation, the morphology and size of the PDA nanoparticles were investigated in solution and on the surface of PVDF films [58]. In solution, the PDA particles' size decreased upon a temperature increase from 20 to 60°C
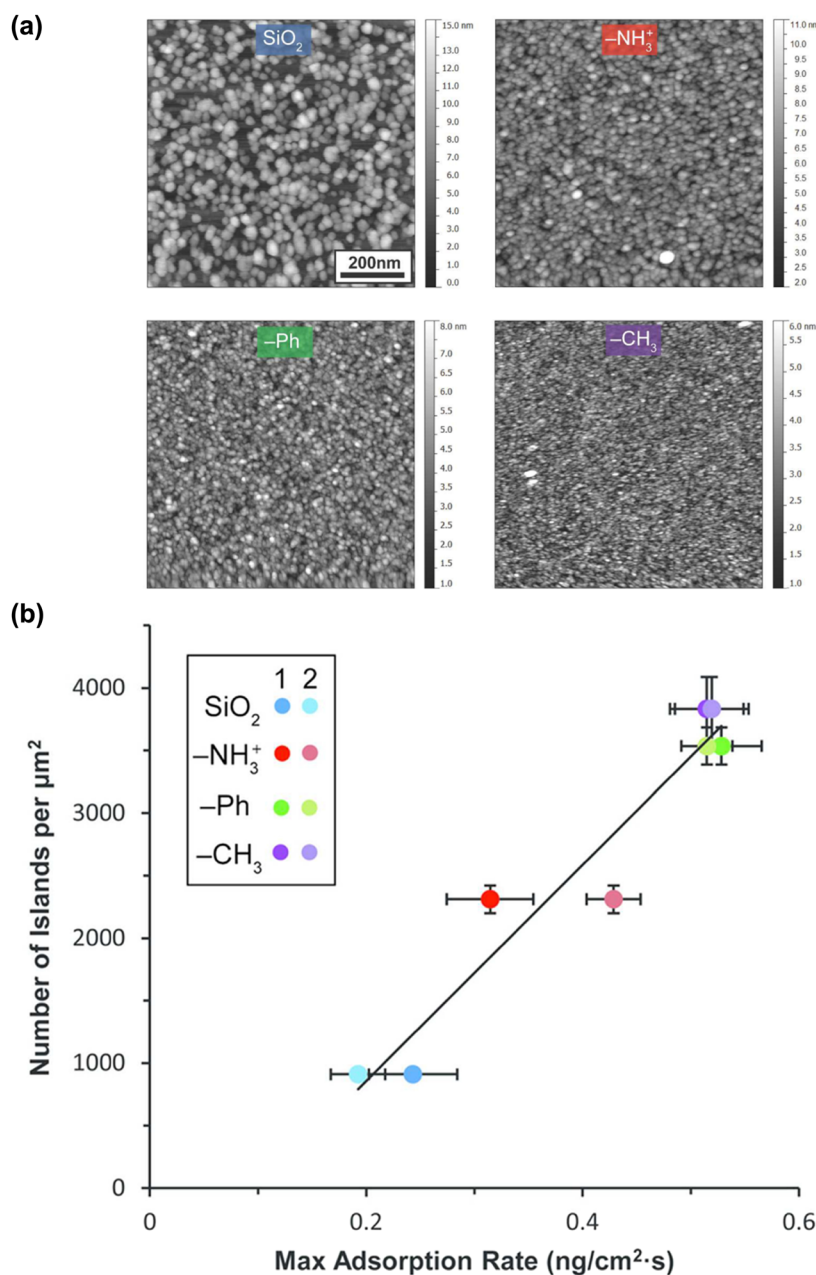
(a)

(b)

Figure 6: (a) AFM surface topographies (image size 0.83 μm × 0.83 μm) of PDA films on substrates terminated with different groups as indicated in the insets. Films were deposited from dopamine solutions at 2 mg mL^{-1} in the presence of 50 mM carbonate/bicarbonate buffer (pH = 8.5) for 24 h. (b) Island density as a function of the maximal adsorption rate measured by quartz crystal microbalance. Reproduced with authorization from [57].

whereas it was almost unaffected on the surface of the deposited PDA film.

The deposition rate, the XPS, and infra-red spectra of PDA films deposited on Au, SiO$_2$, or TiO$_2$ have been investigated in a detailed manner [60,61]. The initial growth rate of PDA, as measured by ellipsometry and by XPS, is faster on gold than on SiO$_2$ and on TiO$_2$ (Figure 7a). The N1s high-resolution XPS spectra on the SiO$_2$ and TiO$_2$ substrates are also markedly different from the spectra obtained on Au after a few minutes of deposition. But after 10–20 min of contact with the dopamine solution, the composition of the PDA films becomes almost substrate independent (Figure 7) [60]. The finding that a deposition time of about 10 min allows for a transition of a substrate-dependent deposition process to the occurrence of a typical "universal" PDA deposition is in agreement with the findings made by Tarlov *et al.* [59].
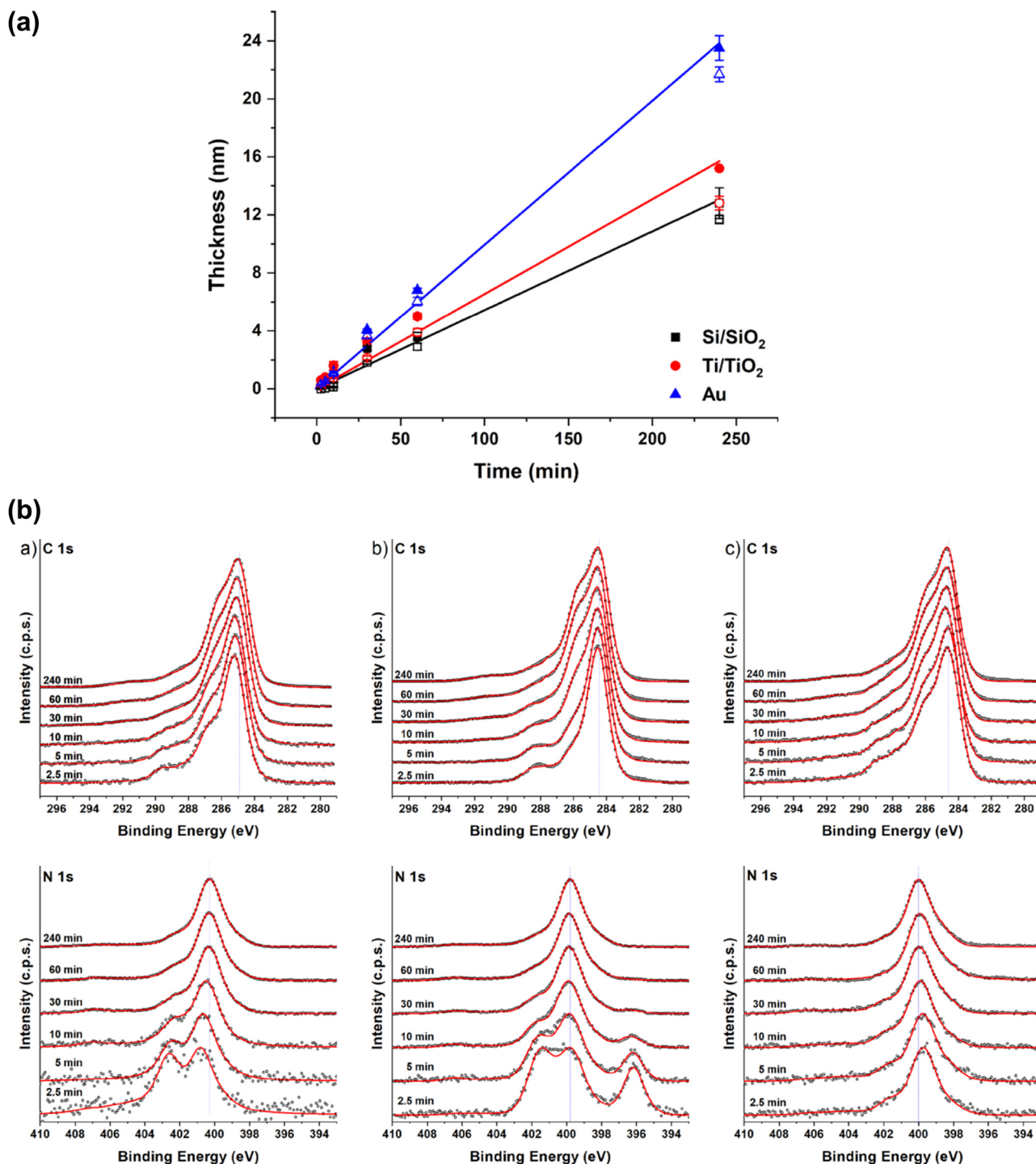
(a)

(b)

Figure 7: (a) Thickness of PDA films on Si/SiO$_x$ (black squares), N-TiO$_2$ (red circles), and Au (blue triangles) substrates as a function of time. The thicknesses were determined by spectroscopic ellipsometry (full symbols) and XPS (empty symbols). (b) (High-resolution C 1s and N 1s XPS spectra of PDA layers formed on Si/SiOx (a), N-TiO$_2$ (b), and Au (c) substrates after 2.5, 5, 10, 30, 60, and 240 min of polymerization in the presence of Tris buffer. The points represent measured and the lines correspond to fitted spectra). Reproduced from [60] with authorization.

The infra-red spectra of the PDA films were also analyzed in detail using principal component analysis [61] with the same conclusion.

These particularly interesting findings incite to ask some fundamental questions about the universality of surface coatings with PDA. It is clear that PDA can be

deposited on all kinds of interfaces, including the air–water interface (Section 2 of the present article) and the interface between some biomolecules or synthetic polymers and water (Section 3 of the present article); however, one may wonder, based on the previously described examples, if all these PDA coatings are strictly identical.

Finally, the surface of particles made from the oxidation of DHI is able to induce further deposition of material on the particles surface when non-oxidized DHI is added in the nanoparticle-containing suspension [53].

PDA films having reached their maximal thickness (about 45 nm after 16 h of deposition on silicon slides) continue to grow when fresh non-oxidized dopamine is added in the presence of Tris buffer (pH = 8.5) and dissolved O_2 [18] provided the film resulting from a previous deposition step is dried before contact with a new dopamine solution. After 7 successive deposition steps lasting over 8 h per deposition step, the PDA film (on a silicon wafer) reached a final thickness of 270 nm as determined by ellipsometry [18]. This result, as the one obtained by Arzillo *et al.* [53], means that the PDA–solution interface is amenable to PDA deposition as any other kind of solid–liquid interface. It has also to be noted that in many instances, the PDA film has reached its saturation value on silicon oxide delaminates from that substrate [18]. This is not the case on other substrates and highlights that the adhesion strength of PDA may be substrate dependent as suggested from AFM measurements where the tip at the extremity of the cantilever has been modified with dopamine and brought in contact with different kinds of solid surfaces [62]. Such substrate-specific adhesion strength should be investigated more systematically in future studies.

In addition, when boric acid is added to the dopamine solution during the deposition of the PDA film, its growth is inhibited due to the strong coordination of boric acid on the catechols at the PDA–solution interface impeding further deposition at this interface [63]. The strong hydrogen bonds coordination between dopamine and tetraborate can hence be used to fine-tune the size and the thickness of PDA nanoparticles and films, respectively [64].

Comparatively to interfaces with an infinite radius of curvature (but nevertheless displaying some roughness) the deposition of PDA on highly curved interfaces or in confined media has been poorly investigated. PDA can be deposited not only at the interface between polyelectrolyte multilayer films, obtained through the alternated deposition of oppositely charged polyelectrolytes [65], and the dopamine solution, but also in the internal pores of the multilayered films [66,67] modifying the mechanical properties as well as the permeability of those coatings towards redox probes.

When L-DOPA is intercalated in zeolite beta and if the pH remains unchanged (equal to 5.9) its oxidation leads to the formation of dimers where the carboxylates are protonated [68]. This result is consistent with the findings reported for the oxidation of DHI and 5,6-dihydroxy-1-methylindole (MDHI) in the 0.7 nm pores of zeolite L [69]. The oxidation product was red and its characterization after dissolution of the zeolite allowed to show the presence of a molecule displaying an m/z value of 337 in mass spectrometry. This value corresponds to an indole dimer in which the indole units are linked in the 2 position, i.e., through the carbon atoms vicinal to the nitrogen, as shown by CP/MAS ^{13}C NMR spectroscopy. When DHI and MDHI are encapsulated in the larger pores (10.8 nm in diameter) of the SBA-15 mesoporous silica, the oxidation product is black, which is consistent with the formation of a eumelanin material [69]. These two investigations [68,69] show that the oxidation of L-DOPA and DHI in constrained volumes is limited to the formation of dimers and the evolution thereof in eumelanin-like or PDA-like material requiring pore volumes larger than a few nanometers.

The oxidation of L-DOPA in slightly basic conditions is different in the presence of Laponite containing exposed Mg^{2+} cations [70] and in the presence of Saponite containing Al^{3+} cations in its tetrahedral sheets [71], such cations being absent in Laponite. In particular, in the presence of Laponite, a eumelanin-like material is formed around the clay and the whole reaction medium is gelified [70]. NMR data suggested that the L-DOPA moieties in the obtained material underwent some decarboxylation [70]. The Mg^{2+} cations in Laponite are suspected to play a catalytic role in the oxidation of L-DOPA and hence in the formation of a PDA-like material around the smectite template.

When dopamine is oxidized in the presence of PET foils carrying a unique channel and having an initial diameter of around 900 nm, transmembrane ion currents decrease progressively after 2 h of dopamine oxidation. The corresponding effective pore radius after this reaction time is of the order of 200 nm [72]. The non-modified micropore displayed a pure ohmic behavior in its ionic conductivity but the deposition of PDA on the pore walls, explaining the decrease of its effective radius, allowed for a rectification, namely a pH-dependent ionic selectivity of the pore channel (Figure 8A). At pH values below the isoelectric point of PDA (estimated here between pH = 4 and pH = 6, in good agreement with planar PDA films deposited in the same experimental conditions but on silica [73]), the PDA film is positively charged (Figure 8A(a)) and displays selective conductivity for anions (Figure 8A(b)) with a positive rectification rate (Figure 8A(c)). However, above the
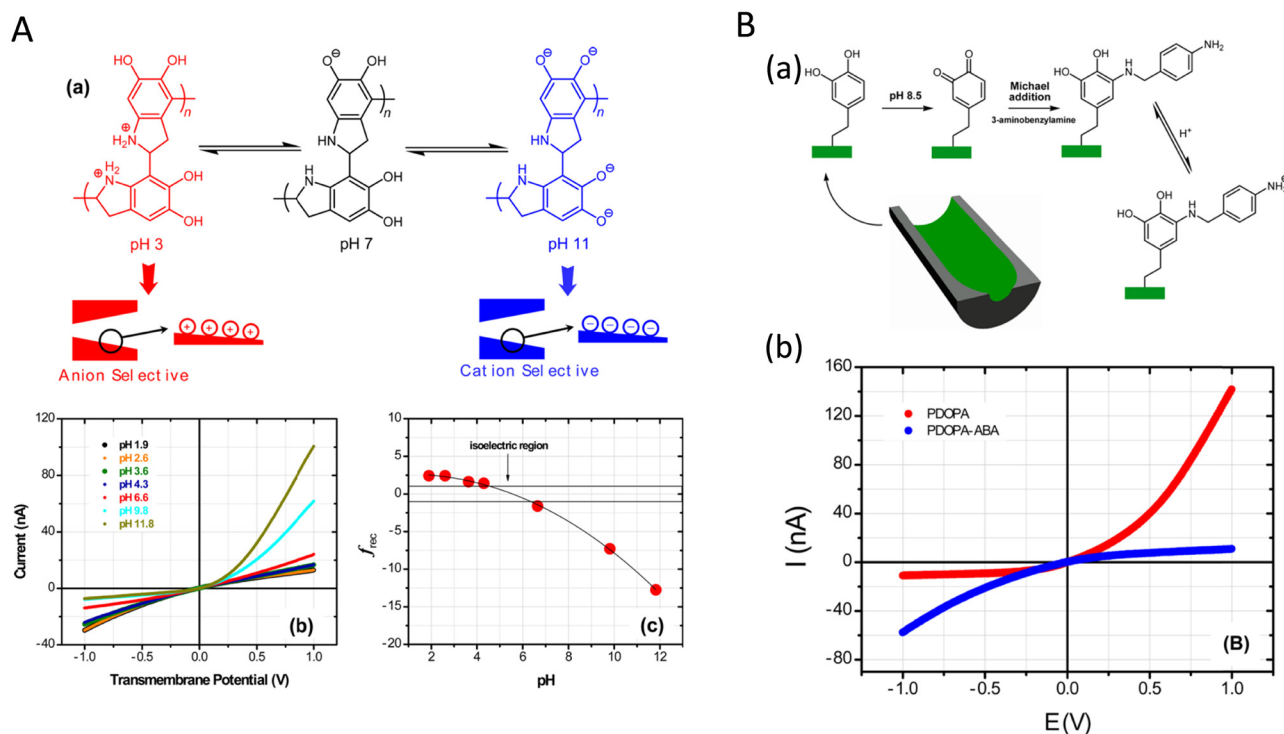
Figure 8: (A) (a) Scheme representing the ionization state of PDA as a function of the solution pH and its influence on the surface charge of a single channel etched in a PET foil. (b) pH influence of the *I–V* characteristics of the PDA-coated nanochannel and (c) rectification ratio of the nanochannel as a function of the pH. These data show a transition from an anion-selective channel to a cation-selective one upon crossing the isoelectric point of the PDA coating covering the internal walls of the channel. (B) (a) Post-functionalization of the PDA-coated channel with 4-aminobenzylamine and its influence on the ion selectivity of the nanochannel. Modified from [72] with authorization.

isoelectric point, the negatively charged PDA layer (Figure 8A(a)) is selective for cations (Figure 8A(b)) and displays a negative rectification rate (Figure 8A(c)). The ion selectivity can also be modified at a constant pH value but after modification of the deposited PDA with 4-aminobenzylamine (Figure 8B).

When the outer membrane pore-forming protein F (Ompf) is inserted in a supported lipid bilayer membrane, the ionic conductance through the tree pores of the trimeric protein decreases up to complete closure when dopamine is added in oxidizing conditions on one side of the lipid bilayer [74]. In addition, PDA not only forms in the pores of Ompf but also on the lipid bilayer and increases its stability against rupture induced by electric pulses: in the absence of PDA the bilayer (made from 1,2-diphytanoyl-sn-glycero-3-phosphatidylcholin) ruptures on average upon application of a transmembrane potential of about 200 mV, but after 2–4 h of PDA deposition (either at pH = 8.5 using dissolved O_2 as the oxidant or at pH = 5 using $NaIO_4$ as the oxidant) the membrane is stable up to 1 V of transmembrane potential [74]. In addition, the PDA-stabilized bilayer keeps its integrity (i.e., it remains insulating) upon the addition of

Triton X100 at 1 μM, a surfactant concentration high enough to destabilize an unmodified bilayer [74].

Finally, Lee *et al.* showed the absence of PDA film deposition on silica in the presence of a DMSO-containing solution [26]. It has to be asked if this absence of apparent film deposition is intrinsic to that solvent-substrate combination or if the obtained coatings delaminate from the substrate, as has been observed (but not systematically) at the silicon–water interface [18].

5 The interface between PDA and water

PDA films deposited on many substrates from an aerated Tris buffer at pH = 8.5 display a static water contact angle of about 45–50° and a constant O/C ratio of 0.13 as determined by XPS [3]. This finding suggests a constant PDA-solution interface despite a wide variation of the substrate–water interface before PDA deposition. However, changing

the oxidation method of dopamine results in a wide variation in the film roughness, its static water contact angle, and composition [75]. In the presence of strong oxidants, like sodium periodate, ammonium peroxodisulfate, or a mixture of copper sulfate and hydrogen peroxide, the O/C ratio of the PDA films (deposited on Au to avoid any contribution of O atoms originating on oxide surfaces) is significantly higher than the O/C ratio of dopamine. This shows that the oxidant not only oxidizes dopamine but also the obtained PDA. Consequently, the PDA films become more hydrophilic and even superhydrophilic [16]. This means that the composition and the structure of the PDA–solution interface can be easily tuned.

6 Conductive surfaces as oxidants in the electropolymerization of PDA

The oxidation of dopamine or other catecholamines in solution yields to deposition of films at the solid–water

and air–water interfaces (depending on the shear stress imposed during the stirring of the solution) but also to the formation of precipitates (or nanomaterials) in solution. In most of the cases, the formation of the PDA precipitate in solution is a drawback because of losing the majority of the used precursors. To deposit similar films without waste of dopamine, its electrical oxidation is a method of choice. Of course, it can only be implemented on conductive substrates. Many papers describe the formation of PDA-like films from dopamine [76–80] or from related molecules [81] containing solutions.

Via pulsed electrochemical deposition, PDA coatings of about 70 nm in thickness could be obtained after 90 pulse cycles from a dopamine solution at $1 \, mg \, mL^{-1}$ (in deoxygenated phosphate buffer at pH = 7.4) on a Pt ultramicroelectrode electrode [82]. This film thickness is much higher than the value obtained by immersing a Pt surface in a dopamine solution using dissolved O_2 as the oxidant [3].

On amorphous carbon surfaces the permeability of PDA films towards hexacyanoferrate anions depends markedly on the deposition method (Figure 9) from dopamine solutions at pH = 8.5 in the presence of Tris buffer [83].

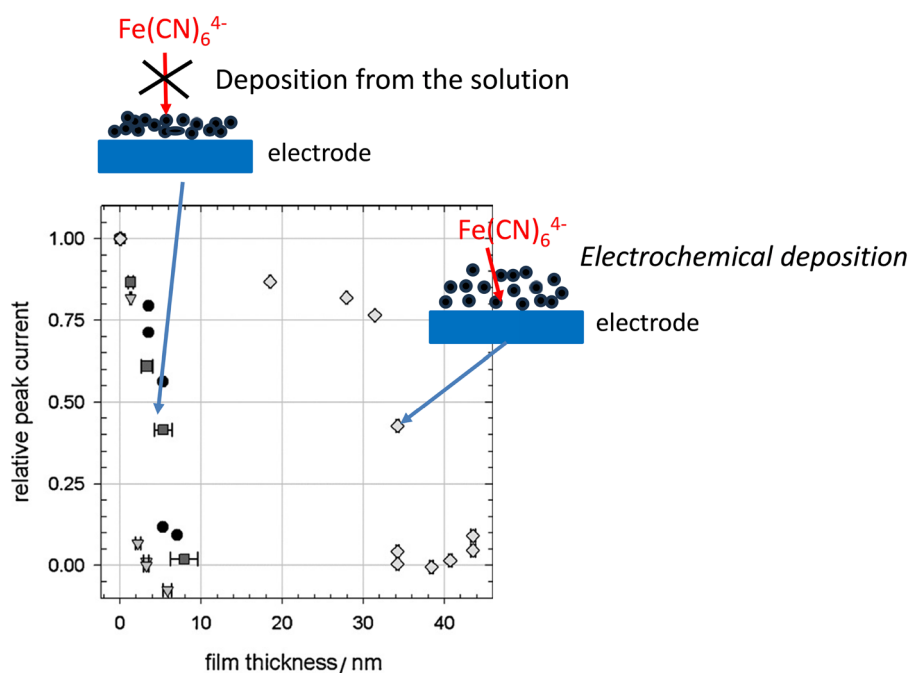**Figure 9:** Relative peak currents of potassium hexacyanoferrate (1 mM in presence of Tris–NaNO$_3$ buffer) *versus* thickness of PDA deposits on the working electrode obtained by methods A (black disks, repetitive injections of $2 \, mg \, mL^{-1}$ dopamine solutions freshly prepared in Tris buffer at pH = 8.5), B (triangles, unique immersion of the electrode in a $2.0 \, mg \, mL^{-1}$ dopamine solution in Tris buffer at pH = 8.5), C (gray squares, 30 mM CuSO$_4$ added to the dopamine solution at $2.0 \, mg \, mL^{-1}$ just before immersion of the working electrode, the pH being close to 4.5), or D (◆, films prepared from nitrogen purged $2.0 \, mg \, mL^{-1}$ dopamine solutions in Tris buffer + 150 mM NaNO$_3$ at pH = 8.5 by successive CV scans at $10 \, mV \, s^{-1}$). Each point corresponds to an experiment performed on an independent electrode modified by a PDA film. The scheme represents the hypothetical porosity of the solution deposited and the electrochemically deposited PDA films and its influence on the permeation of hexacyanoferrate anions. Reproduced with authorization from [83].

The PDA films deposited from successive cyclic voltammetry scans (potential sweep rate: 10 mV s^{-1}) seem to be permeable up to their maximal thickness (about 40 nm as calculated from electrochemical quartz crystal microbalance experiments) whereas those deposited by the solution method become impermeable above 10 nm in thickness. The same holds true for the films deposited using Cu^{2+} cations as the oxidant (Figure 9). These findings strongly suggest, but are not a proof, that controlling the oxidation of dopamine from the solid–liquid interface could allow to modify the porosity and eventually the structure of PDA coatings. More investigations should be performed on the influence of the electrode material on the electrochemical deposition of dopamine and related molecules (either by cyclic voltammetry or by chronoamperometry) owing to the well-known electrode-dependent electron transfer processes, which could in turn change the whole mechanism of PDA formation (made of electrochemical and non-electrochemical steps).

PDA films produced by cyclic voltammetry and detached from the electrode by a poly(vinyl alcohol)-based method [84] display mechanical properties (in terms of elastic modulus) comparable to PDA-free standing films from the air–water interface [32].

Very recently, the surface-controlled electrodeposition and the deposition in a mesoporous environment have been combined [85]. The pH-dependent permselectivity found in the PDA decorated micro-channels [72] was also observed in PDA electrodeposited films on silica A and silica B type films with respective pore diameters around 5 and 7 nm, respectively [85]. The mesoporous material was deposited on an ITO working electrode.

7 Conclusions

In this review article, the state of knowledge in some subtle influences of interfaces on the deposition kinetics, composition, and structure of PDA films has been described. Those findings highlight the above well-established universal nature of PDA coatings; some influence of the particular interface exists. Those effects are spectacular on air–water interfaces when compared with solid–water interfaces, but even at the latter, the particular chemistry of the interface seems to influence the initial steps of PDA deposition. From all these experiments, which need to be completed by additional investigations, an assumption is made herein; PDA films become surface independent (under given physicochemical conditions in the solution,

namely for a given pH, oxidant, and dopamine concentration) only when the substrate-dependent coating accumulates sufficient small PDA clusters from the solution. At the initial stages of the deposition process, the surface adsorbs the oxidized species from the solution presenting the highest affinity for that particular interface. It has to be noted that almost all researchers in this field make the assumption that PDA precursors in the solution deposit on the surface, not only through physisorption but also possibly through chemisorption (if the solid substrate carries some nucleophilic groups). The possibility that a surface-guided polymerization or self-assembly from those adsorbed species could occur is totally neglected. Such a surface-specific effect could explain that, at least in the initial steps of the deposition, some additional substrate specificity occurs because the activation energy of some chemical pathways could be totally different on a solid substrate than in the bulk of the solution, or on another material.

Owing to the findings reviewed herein and to the already known influence of solution conditions on the fate of PDA formation, it could be suggested to explicit the nomenclature used to design the obtained PDA-based materials as already suggested previously [86] but in a somewhat more complete manner. This nomenclature, which should be discussed in the research community working in this field, could be the following: poly(monomer)@substrate@oxidant + additives. For instance, a film produced at the air–water interface from a dopamine solution in the presence of sodium periodate and in the presence of PEI should be called: poly(dopamine)@air@NaIO$_4$ + PEI. This is of course only a superficial indication, because the reaction time, the pH, and the temperature are not specified, but it would allow to immediately distinguish the obtained material from the poly(dopamine)@silica@O$_2$, which are the most frequently investigated PDA films and which are clearly different than the poly(dopamine)@air@NaIO$_4$ + PEI films as reviewed herein.

Conflict of interest: The author states no conflict of interest.

References

[1] Ulman A. Formation and structure of self-assembled monolayers. Chem Rev. 1996;96:1533–54.

[2] Sagiv JJ. Organized monolayers by adsorption. 1. Formation and structure of oleophobic mixed monolayers on solid surfaces. Am Chem Soc. 1980;102:92–8.

[3] Lee H, Dellatore SM, Miller WM, Messersmith PB. Mussel-inspired surface chemistry for multifunctional coatings. Science. 2007;318:426–30.

[4] Lee BP, Messersmith PB, Israelachvili JN, Waite JH. Mussel-inspired adhesives and coatings. Ann Rev Mater Res. 2011;41:99–132.

[5] Liu Y, Ai K, Lu L. Polydopamine and its derivative materials: synthesis and promising applications in energy, environmental, and biomedical fields. Chem Rev. 2014;114:5057–115.

[6] Barclay TG, Hegab HM, Clarke SR, Ginic-Markovic M. Versatile surface modification using polydopamine and related polycate-cholamines: Chemistry, structure, and applications. Adv Mater Interf. 2017;4:art. 1601192.

[7] Lee H, Rho J, Messersmith PB. Facile conjugation of biomolecules onto surfaces *via* mussel adhesive protein inspired coatings. Adv Mater. 2009;21:431–4.

[8] Kang SM, Rho J, Choi IS, Messersmith PB, Lee H. Norepinephrine: material-independent, multifunctional surface modification reagent. J Am Chem Soc. 2009;131:13224–25.

[9] Zhu J, Edmondson S. Polydopamine-melanin initiators for Surface-initiated ATRP. Polymer. 2011;52:2141–9.

[10] Farnad N, Farhadi K, Voelcker NH. Polydopamine nanoparticles as a new and highly selective biosorbent for the removal of copper (II) ions from aqueous solutions. Water Air Sol Pollut. 2012;223:3535–44.

[11] Postma A, Yan Y, Wang Y, Zelikin AN, Tjipto E, Caruso F. Self-polymerization of dopamine as a versatile and robust technique to prepare polymer capsules. Chem Mater. 2009;21:3042–4.

[12] Mrówczyński R, Bunge A, Liebscher J. Polydopamine–an organo-catalyst rather than an innocent polymer. Chem Eur J. 2014;20:8647–53.

[13] Pawar SA, Chand AN, Kumar AV. Polydopamine: An amine oxidase mimicking sustainable catalyst for the synthesis of nitrogen heterocycles under aqueous conditions. ACS Sustain Chem Eng. 2019;7:8274–86.

[14] Du Y, Yang HC, Xu XL, Wu J, Xu ZK. Polydopamine as a catalyst for thiol coupling. ChemCatChem. 2017;7:3822–5.

[15] Molnár Á. Polydopamine – its prolific use as catalyst and support material. ChemCatChem. 2020;12:2649–89.

[16] Ponzio F, Barthes J, Bour J, Michel M, Bertani Ph, Hemmerle J, et al. Oxidant control of polydopamine surface chemistry in acids: A mechanism-based entry to superhydrophilic-superoleophobic coatings. Chem Mater. 2016;28:4697–4705.

[17] Zhang C, Ou Y, Lei WX, Wan LS, Ji J, Xu ZK. CuSO4/H2O2-induced rapid deposition of polydopamine coatings with high uniformity and enhanced stability. Angew Chem Int Ed. 2016;128:3106–9.

[18] Bernsmann F, Ball V, Addiego F, Ponche A, Michel M, de Almeida Gracio JJ, et al. Dopamine-melanin film deposition depends on the used oxidant and buffer solution. Langmuir. 2011;27:2819–25.

[19] Della Vecchia NF, Luchini A, Napolitano A, D'Errico G, Vitiello G, Szekeli N, et al. Tris buffer modulates polydopamine growth, aggregation, and paramagnetic properties. Langmuir. 2014;30:9811–8.

[20] Ball V, Hirtzel J, Leks G, Frisch B, Talon I. Experimental methods to get polydopamine films: a comparative review on the synthesis methods, the films' composition and properties. Macromol Rapid Comm. 2023;44:art.2200946.

[21] Dreyer DR, Miller DJ, Freeman BD, Paul DR, Bielawski BW. Elucidating the structure of poly(dopamine). Langmuir. 2012;28:6428–35.

[22] Liebscher J, Mrówczyński R, Scheidt HA, Filip C, Hădade ND, Turcu R, et al. Structure of polydopamine: A never-ending story? Langmuir. 2013;29:10539–48.

[23] Ryu JH, Messersmith PB, Lee H. Polydopamine surface chemistry: A decade of discovery. ACS Appl Mater Interf. 2018;10:7523–40.

[24] Meredith P, Sarna T. The physical and chemical properties of eumelanin. Pig Cell Res. 2006;19:572–94.

[25] Hong S, Na YS, Choi S, Song IT, Kim WY, Lee H. Non-covalent self-assembly and covalent polymerization co-contribute to polydopamine formation. Adv Funct Mater. 2012;22:4711–7.

[26] Park HK, Park JH, Lee H, Hong S. Material-selective polydopamine coating in dimethyl sulfoxide. ACS Appl Mater Interf. 2020;12:49146–54.

[27] Ponzio F, Payamyar P, Schneider A, Winterhalter M, Bour J, Addiego F, et al. Polydopamine films from the forgotten air/water interface. J Phys Chem Lett. 2014;5(19):3436–40.

[28] Ponzio F, Ball V. Polydopamine deposition at fluid interfaces. Polym Int. 2016;65:1251–7.

[29] Milyaeva OY, Bykov AG, Campbell RA, Loglio G, Miller R, Noskov BA. Polydopamine layer formation at the liquid–gas interface. Colloids Surf A: Physicochem Eng Asp. 2019;579:art 123637.

[30] Abe H, Matsue T, Yabu H. Reversible shape transformation of ultrathin polydopamine-stabilized droplet. Langmuir. 2017;33:6404–9.

[31] Szewczyk J, Pochylski M, Szutkowski K, Kempiński M, Mrówczyński R, Iatsunskyi I, et al. In-situ thickness control of centimetre-scale 2D-Like polydopamine films with large scalability. Mater Today Chem. 2022;24:art 100935.

[32] Coy E, Iatsunskyi I, Colmenares JC, Kim Y, Mrówczyński R. Polydopamine films with 2D-like layered structure and high mechanical resilience. ACS Appl Mater Interf. 2021;13:23113–20.

[33] Rono N, Kibet JK, Martincigh BS, Nyamori VO. A review of the current status of graphitic carbon nitride. Crit Rev Solid State Mater Sci. 2020;46:189–217.

[34] Watt AAR, Bothma JP, Meredith P. The supramolecular structure of melanin. Soft Matter. 2009;5:3754–60.

[35] Chen CT, Ball V, de Almeida Gracio JJ, Singh MK, Toniazzo V, Ruch D, et al. Self-assembly of tetramers of 5,6-dihydroxyindole explains the primary physical properties of eumelanin: experiment, simulation, and design. ACS Nano. 2013;7:1524–32.

[36] Szewczyk J, Babacic V, Krystofik A, Ivashchenko O, Pochylski M, Pietrzak R, et al. Control of intermolecular interactions toward the production of free-standing interfacial polydopamine films. ACS Appl Mater Interf. 2023;15:36922–35.

[37] Han X, Tang F, Jin Z. Free-standing polydopamine films generated in the presence of different metallic ions: The comparison of reaction process and film properties. RSC Adv. 2018;8: 18347–54.

[38] Hong S, Schaber CF, Dening K, Appel E, Gorb SN, Lee H. Air/water interfacial formation of freestanding, stimuli-responsive, self-healing catecholamine Janus-faced microfilms. Adv Mater. 2014;26:7581–7.

[39] Yang HC, Xu W, Du Y, Wu J, Xu ZK. Composite free-standing films of polydopamine/polyethyleneimine grown at the air/water interface. RSC Adv. 2014;4:45415–18.

[40] Ponzio F, Le Houerou V, Zafeiratos S, Gauthier C, Garnier T, Jierry L, et al. Robust alginate-catechol@polydopamine free-standing membranes obtained from the water/air interface. Langmuir. 2017;33:2420–6.

[41] Milyaeva OY, Bykov AG, Campbell RA, Loglio G, Miller R, Noskov BA. Colloids Surf A: Physicochem Eng Asp. 2020;599:art 124930.

[42] Clancy CMR, Simon JD. Ultrastructural organization of eumelanin from Sepia officinalis measured by atomic force microscopy. Biochemistry. 2001;40:13353–60.

[43] Kushimoto T, Basrur V, Valencia J, Matsunaga J, Vieira WD, Ferrans VJ, et al. A model for melanosome biogenesis based on the purification and analysis of early melanosomes. Proc Natl Acad Sci USA. 2001;98:10698–10703.

[44] Guo SL, Hong L, Akhremitchev BB, Simon JD. Surface elastic properties of human retinal pigment epithelium melanosomes. Photochem Photobiol. 2008;84:671–8.

[45] Della Vecchia NF, Cerruti P, Gentile G, Errico ME, Ambrogi V, D'Errico G, et al. Artificial biomelanin: Highly light-absorbing nanosized eumelanin by biomimetic synthesis in chicken egg white. Biomacromolecules. 2014;15:3811–6.

[46] Chassepot A, Ball V. Human serum albumin and other proteins as templating agents for the synthesis of nanosized dopamine-eumelanin. J Colloid Interf Sci. 2014;414:97–102.

[47] Crivellato E, Nico B, Ribatti D. The chromaffin vesicle: advances in understanding the composition of a versatile, multifunctional secretory organelle. Anat Rec. 2008;291:1587–602.

[48] Bergtold C, Hauser D, Chaumont A, El Yakhlifi S, Mateescu M, Meyer F, et al. Mimicking the chemistry of natural eumelanin synthesis: The KE sequence in polypeptides and in proteins allows for a specific control of nanosized functional polydopamine formation. Biomacromolecules. 2018;19:3693–704.

[49] El Yakhlifi S, Ihiawakrim D, Ersen O, Ball V. enzymatically active polydopamine @ alkaline phosphatase nanoparticles produced by NaIO(4) oxidation of dopamine. Biomimetics. 2018;3:art. 36.

[50] Hauser D, Milosevic A, Steinmetz L, Vanhecke D, Septiadi D, Petri-Fink A, et al. Polydopamine/transferrin hybrid nanoparticles for targeted cell-killing. Nanomaterials. 2018;8:art. 1065.

[51] Strube OI, Büngeler A, Bremser W. Site-specific in situ synthesis of eumelanin nanoparticles by an enzymatic autodeposition-like process. Biomacromolecules. 2015;16:1608–13.

[52] Alfieri M-L, NG D, Weil T, Ball V. Polydopamine at biological interfaces. Adv Colloid Interf Sci. 2022;305:art 102689.

[53] Arzillo M, Mangiapia G, Pezzella A, Heenan RK, Radulescu A, Paduano L, et al. Eumelanin buildup on the nanoscale: aggregate growth/assembly and visible absorption development in biomimetic 5,6-dihydroxyindole polymerization. Biomacromolecules. 2012;13:2379–90.

[54] Ponzio F, Bertani P, Ball V. Role of surfactants in the control of dopamine-eumelanin particle size and in the inhibition of film deposition at solid–liquid interfaces. J Colloid Interf Sci. 2014;431:176–9.

[55] Mateescu M, Metz-Boutigue MH, Bertani P, Ball V. Polyelectrolytes to produce nanosized polydopamine. J Colloid Interf Sci. 2016;469:184–90.

[56] Muller C, Berber E, Lutzweiler G, Ersen O, Bahri M, Lavalle P, et al. Front Bioeng Biotech. 2020;8:art.982.

[57] Klosterman L, Riley JK, Bettinger C. Control of heterogeneous nucleation and growth kinetics of dopamine-melanin by altering substrate chemistry. Langmuir. 2015;31:3451–8.

[58] Jiang J, Zhu L, Zhu L, Zhu B, Xu Y. Surface characteristics of a self-polymerized dopamine coating deposited on hydrophobic polymer films. Langmuir. 2011;27:14180–87.

[59] Zangmeister RA, Morris TA, Tarlov MJ. Characterization of polydopamine thin films deposited at short times by autoxidation of dopamine. Langmuir. 2013;29:8619–28.

[60] Svoboda J, Král M, Dendisová M, Matějka P, Pop-Georgievski O. Unravelling the influence of substrate on the growth rate, morphology and covalent structure of surface adherent polydopamine films. Colloids Surf B: Biointerf. 2021;205:art 111897.

[61] Král M, Dendisová M, Matějka P, Svoboda J, Pop-Georgievski O. Infrared imaging of surface confluent polydopamine (PDA) films at the nanoscale. Colloids Surf B: Biointerf. 2023;221:art 112954.

[62] Lee H, Lee BP, Messersmith PB. A reversible wet/dry adhesive inspired by mussels and geckos. Nature. 2007;448:338–41.

[63] Schneider A, Hemmerle J, Allais M, Didierjean J, Michel M, d'Ischia M, et al. Boric acid as an efficient agent for the control of polydopamine self-assembly and surface properties. ACS Appl Mater Inter. 2018;10:7574–80.

[64] Ruppel SS, Liang J. Tunable properties of polydopamine nanoparticles and coated surfaces. Langmuir. 2022;38:5020–9.

[65] Decher G. Fuzzy nanoassemblies: Toward layered polymeric multicomposites. Science. 1997;277:1232–7.

[66] Bernsmann F, Richert L, Senger B, Lavalle P, Voegel JC, Schaaf P, et al. Use of polymerisation to produce free-standing membranes from exponentially growing multilayer films. Soft Matter. 2008;4:1621–4.

[67] Ball V, Apaydin K, Laachachi A, Toniazzo V, Ruch D. Changes in permeability and in mechanical properties of layer-by-layer films made from poly(allylamine) and montmorillonite postmodified upon reaction with dopamine. Biointerphases. 2012;7:art.59.

[68] Bouchoucha M, Tielens F, Gaslain F, Costa Torro F, Casale S, Palcic A, et al. Melanin polymerization held in check: A composite of dihydroxyphenylalanine with zeolite beta. J Phys Chem C. 2015;119:8736–47.

[69] Prasetyanto EA, Manini P, Napolitano A, Crescenzi O, d'Ischia M, De Cola L. Towards eumelanin@zeolite hybrids: Pore-size-controlled 5,6-dihydroxyindole polymerization. Chem Eur J. 2014;20:1597–601.

[70] Jaber M, Lambert JF. A new nanocomposite: L-DOPA/Laponite. J Phys Chem Lett. 2010;1:85–8.

[71] Jaber M, Bouchoucha M, Delmotte L, Méthivier C, Lambert JF. Fate of L-DOPA in the presence of inorganic matrices: Vectorization or composite material formation. J Phys Chem C. 2011;115:9216–25.

[72] Pérez-Mitta G, Tuninetti JS, Knoll W, Trautmann C, Toimil-Molares ME, Azzaroni O. Polydopamine meets solid-state nanopores: A bioinspired integrative surface chemistry approach to tailor the functional properties of nanofluidic diodes. J Am Chem Soc. 2015;137:6011–7.

[73] Ball V. Impedance spectroscopy and zeta potential titration of dopa-melanin films produced by oxidation of dopamine. Colloids Surf A Physicochem Eng Asp. 2010;363:92–7.

[74] Neveshkin A, Citak F, Ball V, Winterhalter M. Polydopamine coating to stabilize a free-standing lipid bilayer for channel sensing. Langmuir. 2017;33:7256–62.

[75] El Yakhlifi S, Alfieri ML, Arntz Y, Eredia M, Ciesielski A, Samori P, et al. The antioxidant activity of polydopamine films prepared from different oxidants is finetuned by their composition and roughness. Colloids Surf A: Physicochem Eng Asp. 2021;614:art. 126134.

[76] Li Y, Liu M, Xiang C, Xie Q, Yao S. Electrochemical quartz crystal microbalance study on growth and property of the polymer deposit at gold electrodes during oxidation of dopamine in aqueous solutions. Thin Solid Films. 2006;497:270–8.

[77] Stöckle B, Wah Ng DY, Meier C, Paust T, Bischoff F, Diemant T, et al. Precise control of polydopamine film formation by electropolymerization. Macromol Symp. 2014;346:73–81.

[78] Vatral J, Boča R, Linert W. Oxidation properties of dopamine at and near physiological conditions. Monatshefte Chem. 2015;146:1799–805.

[79] Li S, Wang H, Young M, Xu F, Cheng G, Cong H. Properties of electropolymerized dopamine and its analogues. Langmuir. 2019;35:1119–25.

[80] Almeida LC, Correia RD, Squillaci G, Morana A, La Cara F, Correia JP, et al. Electrochemical deposition of bio-inspired laccase-polydopamine films for phenolic sensors. Electrochim Acta. 2019;319:462–71.

[81] D'Alvise TM, Sunder S, Hasler R, Moser J, Knoll W, Synatscke CV, et al. Macromol Rapid Comm. 2022;art. 2200332.

[82] Lin J, Daboss S, Blaimer D, Kranz C. Micro-structured polydopamine films *via* pulsed electrochemical deposition. Nanomaterials. 2019;9:art. 242.

[83] Bernsmann F, Voegel JC, Ball V. Different synthesis methods allow to tune the permeability and permselectivity of dopamine–melanin films to electrochemical probes. Electrochim Acta. 2011;56: 3914–9.

[84] D'Alvise TM, Harvey S, Hueske L, Szelwicka J, Veith L, Knowles TPJ, et al. Ultrathin polydopamine films with phospholipid nanodiscs containing a glycophorin A domain. Adv Funct Mater. 2020;30:art. 2000378.

[85] Varol HS, Herberger T, Kirsch M, Mikolai J, Veith L, Kannan-Sampathkumar V, et al. Electropolymerization of polydopamine at electrode-supported insulating mesoporous films. Chem Mater. 2023;35:9192–207.

[86] d'Ischia M, Napolitano A, Ball V, Chen CT, Buehler MJ. Polydopamine and eumelanin: From structure-property relationships to a unified tailoring strategy. Acc Chem Res. 2014;47:3541–50.